Renewable and Sustainable Energy Reviews 149 (2021) 111357

Contents lists available at ScienceDirect

Renewable and Sustainable Energy Reviews

journal homepage: www.elsevier.com/locate/rser

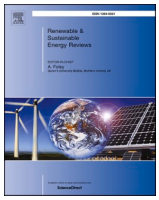

Innovative regression-based methodology to assess the techno-economic performance of photovoltaic installations in urban areas

Enrique Fuster-Palop [a], Carlos Prades-Gil [b], X. Masip [b], Joan D. Viana-Fons [a], Jorge Payá [a,*]

[a] Instituto Universitario de Investigación en Ingeniería Energética, Universitat Politècnica de València, Camino de Vera s/n, Edificio 8E semisótano frente acceso J, Valencia, 46022, Spain
[b] IMPACT-E, C/ Joan Verdeguer n°16, Valencia, 46024, Spain

ARTICLE INFO

Keywords:
Photovoltaics
Self-consumption
Techno-economical assessment
Economic potential
Simplified regression model
Multi-storey residential buildings

ABSTRACT

Households present a significant contribution in the national energy consumption, and photovoltaics (PV) has become an economically feasible technology that can play an important role to lower this consumption and the associated emissions. Nevertheless, there is still a gap between too in-depth technical models for detailed studies and what urban energy planners need, which are simpler, yet reliable techno-economical tools to select which roofs of city buildings are the best candidates for PV production. In order to face this gap, a multiple linear regression (MLR) model has been developed to determine the economic payback using dimensionless parameters. The methodology has been adopted in the city of Valencia (Spain) for a large sample of multi-storey buildings, which are the most common typology. The approach has a high replicability since it can be applied for different countries. The MLR model provides a payback root mean squared error (RMSE) of 0.48 years in comparison with a complex techno-economic model which was previously developed and validated with the software System Advisor Model (SAM). The variables which have a bigger weight in the payback are the shadow losses and the power unit cost due to the economy of scale. With the current Spanish regulation, PV installations on multi-storey buildings can reach paybacks of around 7–15 years and the best option is to have large economies of scales together with a low energy surplus.

1. Introduction

European (EU-28) households accounted in 2018 for 24% (3299 TWh) of the total final energy consumption, and the electricity share was of 25% (811 TWh) [1,2]. This share can be even bigger in some countries, such as in Spain, where 44% was reached (75 GWh) in 2018 [3], and the expectations are that the energy consumption will increase even further [4].

The PV sector is nowadays in a very favorable situation both technically and legally [5], particularly in Spain. The wide solar resource and the high PV penetration has led to a reduction of costs up to 90% during the last decade [6]. Self-consumption has also been promoted throughout the current Spanish regulation with the Royal Decree-Law 15/2018 [5] and the Royal Decree 244/2019 [6], hereby opening the possibility to install PV installations on rooftops of urban environments from which several consumers, such as community of neighbours, can benefit.

However, the scarce awareness of home-owners and investors on the cost-effectiveness of PV facilities has become an important barrier which hinders the implementation of PV facilities in cities [7]. Therefore, for a further penetration of PV in urban areas, a favorable framework is necessary, as well as the development of holistic energy plans. All the energy actors need information both on technical and on economical aspects [8].

In this context, there is a need for tools to analyze the PV economic potential [9] both accurately and with a low computational cost. These models could help energy planners, local administrations, companies, or investors to identify the urban rooftops where PV facilities would present reduced payback periods, and which are consequently more attractive for end users [10].

Literature on accurate PV models on an urban scale is abundant and includes the physical, geographic, as well as the technical PV potential. The most common approach of solar resource assessment in urban environments is based on top-down methods which require to filter the information from radiation timeseries, Laser Imaging Detection and Ranging (LiDAR) and raster or vectorial maps to obtain mainly the solar energy potential on tilted surfaces of rooftops [11] and facades [12].

* Corresponding author.
E-mail address: jorge.paya@iie.upv.es (J. Payá).

https://doi.org/10.1016/j.rser.2021.111357
Received 7 December 2020; Received in revised form 20 April 2021; Accepted 10 June 2021
Available online 3 July 2021

Abbreviations

GIS	Geographic Information System
CO2	Carbon dioxide
LiDAR	Light Detection and Ranging o Laser Imaging
GWh	Gigawatt hour
MLR	Multiple linear regression
kg	Kilogram
PV	Photovoltaic
km	Kilometer
REE	Red Eléctrica de España
kW	Kilowatt
SAM	System Advisor Model
kWh	Kilowatt hour
kW_p	Kilowatt peak
m^2	Square meter
°C	Degree Celsius
t	Ton
TWh	Terawatt hour
V	Volt

Symbol description

W_p	Watt of peak power
BPR	Building Power Ratio
CR	Cost ratio
E_{PV}	Yearly PV production–
$E_{PV,\ location}$	Yearly PV production per power installed in a specific location
$E_{PV,\ building,\ location}$	Yearly PV production in a specific building in a specific location
$E_{PV,\ building,\ Valencia}$	Yearly PV production in a specific building of Valencia
$G_{0,location}$	Yearly global horizontal irradiation
MAE	Mean Absolute Error–
NOCT	Normal Operating Cell Temperature–
P_{PV}	PV Installed Peak Power–
PR	Performance Ratio
R^2	R squared or coefficient of determination–
RMSE	Root mean squared error–
S_{PV}	Yearly PV surpluses
SF	Shading Factor
SL	Shadow Losses–
SR	Surpluses Ratio–
SR*	Surpluses Ratio obtained with the Building Power Ratio
SVF	Sky View Factor–
$T_{0,location}$	Yearly mean ambient temperature–

Some well-known computational radiation models for this purpose are r.sun, ArcGIS Solar Analyst, SolarFlux and SORAM [13]. Additionally, many models has been proposed to estimate the technical PV potential [14], based on manufacturer data such as the module efficiency and the performance ratio (PR). A further level of detail has also been reached by including more complex electrical calculations which have achieved a very good agreement with measurement data [15]. As a result, several recent studies have helped to locate the most productive rooftops in cities such as Irun [16] or Vitoria [17]. Such studies are based on LiDAR and cadastral data and using Geographic Information System (GIS) software tools, which are widely used for this purpose. However they do not adddress cover the economic impact.

Literature regarding the economic feasibility of PV installations in urban areas is very scarce and most frequent models that calculate the energy and economic savings are complex. For instance, Michael J. Mangiante et al. [18] proposed a method that couples geospatial (with LiDAR data) and economic models to determine the size and location of PV facilities on residential rooftops. Ali Mohammad Shirazi et al. [19] carried out a 3D-based techno-economic analysis of the PV potential, and optimized the payback period with the tilt angle of panels for facades and roofs. Commercial software, such as PVsyst [20], TRNSYS [15] or SAM [21], has also been employed to simulate specific PV facilities. Nevertheless, the computational cost would be unassumable if the latter simulation tools were employed on an urban level. Furthermore, such tools do not consider systematically the available surface on rooftops nor the potential shadows cast by the urban environment. The shadowing elements have to be introduced one by one by the user.

For energy planning applications, such as the search of optimal rooftops for PV facilities with a minimum economic payback, detailed results of the PV production are not required and they imply a high computational cost. In an effort to simplify the above-mentioned methods and their high computational demand, several studies carried out bottom-up approaches based on the statistical analysis of the different input variables. Machine learning techniques have also been commonly employed for this purpose [22]. Nevertheless, most frequent machine learning models such as random forest and neural networks add a further complexity in their interpretation and hinder their replicability [23]. In this context of urban planning, one of the simplest, yet fastest, and easy-to-replicate statistical model is a linear regression. Calcabrini et al. [24] proposed a simplified MLR model to estimate the yearly energy yield of PV facilities in urban environments based on a correlation between the radiation components and the skyline profile. The results were accurately validated with measurement data from several facilities. This work is in turn based on a study carried out by Chatzipoulka et al. [25] where the PV production was highly correlated for certain latitudes with the sky view factor (SVF) as a predictor. In contrast with the previous models that require a calculation of the sky view factor, K. H. Poon et al. [26] suggested a MLR model to predict the irradiation on rooftop and facades based on predictors such as the height of the building, the slenderness and the plot ratio. Trigo-Gonzalez et al. [27] proposed a MLR model to predict the hourly PV production using minimum weather conditions and the performance ratio as predictors. With this approach, root mean squared errors (RMSE) lower than 16% were obtained in comparison with measured production data of different PV power plants. Other MLR models employ as predictors technoeconomic, socio-demographic and building variables. For example, the model proposed by Jonas Müller et al. [28] forecasts spatial projections of PV installations, showing the versatility and effectiveness of a multidisciplinary approach.

Nevertheless, the above-mentioned regression models focus on providing a quick estimation of the PV energy production and no additional simplified models have been found to obtain the profitability results, for instance the economic payback of any PV facility on a rooftop of a building. The latter depends on global building features that are easily known in advance, such as the amount of shadow losses or the maximum installable capacity. Consequently, there is a potential to develop simplified models based on the global building characteristics.

In order to cover this gap, the present work provides a regression model to estimate the economic payback. The proposed model is an alternative to the complex top-down models, providing clear information to the local energy planners and the rest of energy actors on the payback which can be obtained with PV installations on a large number of urban rooftops.

Given the previous literature review, the current study presents the following novelties:

- A new MLR methodology has been conceived for the simulation of PV panels in urban areas, considering both the technical and the economic performance, predicting the economic payback of PV facilities on rooftops as a function of the shadow losses, the installed capacity and unit costs.
- A MLR approach has been developed to ensure a high replicability of the methodology in different countries, with their corresponding prices and electricity tariffs.

2. Methods

2.1. Description of the methodology

The present section summarizes the methodology which has been applied to obtain the correlations. As mentioned above, the primary objective of this article is the development of a MLR economic model capable of providing the same global results as more complex and detailed models. Fig. 1 shows the workflow which has been adopted.

In the first place, a complex techno-economic model has been built to calculate the economic payback automatically for any rooftop PV facility defined only by its coordinates. This helps to easily carry out an analysis on an urban scale without going into any further technical details. This model has been in turn validated by comparing the results with the software SAM [29]. In the second place, the predictive variables of the regression model have been identified by analyzing the results of the complex model. In the third place, the sample size has been defined through an iterative process, which starts from a reduced random sample of buildings. The minimum size to obtain a representative regression has been verified by means of an F-test. Finally, in step 4, the paybacks predicted by the MLR model have been compared against the paybacks obtained with the techno-economic model. Furthermore, alternative regressions have been developed to estimate the PV production in other regions of the world based on simple predictors such as shadow losses, installed power, annual horizontal radiation, and mean temperature. These models have been validated with the production obtained from the techno-economic model.

As stated by Campos Inês et al., multi-storey residential buildings present a high potential for electricity savings [30], and they are also the most common buildings in cities by far. Consequently, this typology (urban houses with more than two floors) has been chosen for the present study. Tillmann Lang et al. [31] also stated that large-residential multi-floor buildings provide promising combinations of key drivers of economic performance, in a study which compared the PV self-consumption of four buildings types (residential and commercial, each small and large).

2.2. Techno-economic model

The techno-economic model has been developed in the R programming code to estimate the PV electricity generation and to calculate the energy, economic and environmental impact. The calculations are carried out with an hourly time step. The approach only requires as main input the rooftop coordinates of the building under study.

As shown in Fig. 2, the model is composed of several submodules. In (i) the urban spatial model helps to obtain the skyline of surrounding obstacles around the point of study using LiDAR and cadastral data. In (ii) the irradiation model enables the calculation of the irradiation on a tilted surface considering nearby shadows. In (iii) the production model is employed to calculate the electrical PV yield of the entire facility. In (iv) the electrical demand of the building is calculated and compared with the production. In (v) the economic model estimates the costs, cash flows and energy savings. Finally, in (vi) the emissions model is used to quantify the environmental impact of the facility.

The calculations are particularized to each specific building by using the LiDAR and cadastral information according to the following three variables: the skyline of the surrounding buildings, the rooftop area and the electrical demand of the building.

The techno-economic model is explained in more detail in recent literature [32]. The present section describes the main assumptions and inputs which have been considered.

2.2.1. Spatial urban model

The shadow modelling can be based on shadow profiles or based on the skyline/viewshed. The first method is computationally heavy since it

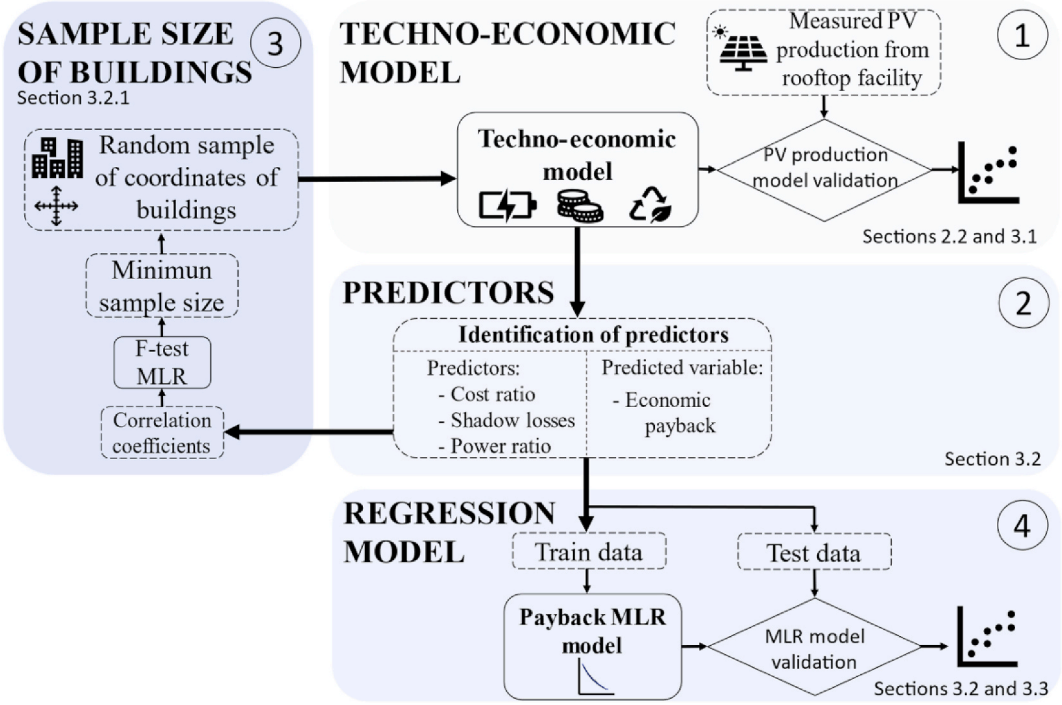

Fig. 1. Workflow of the proposed methodology.

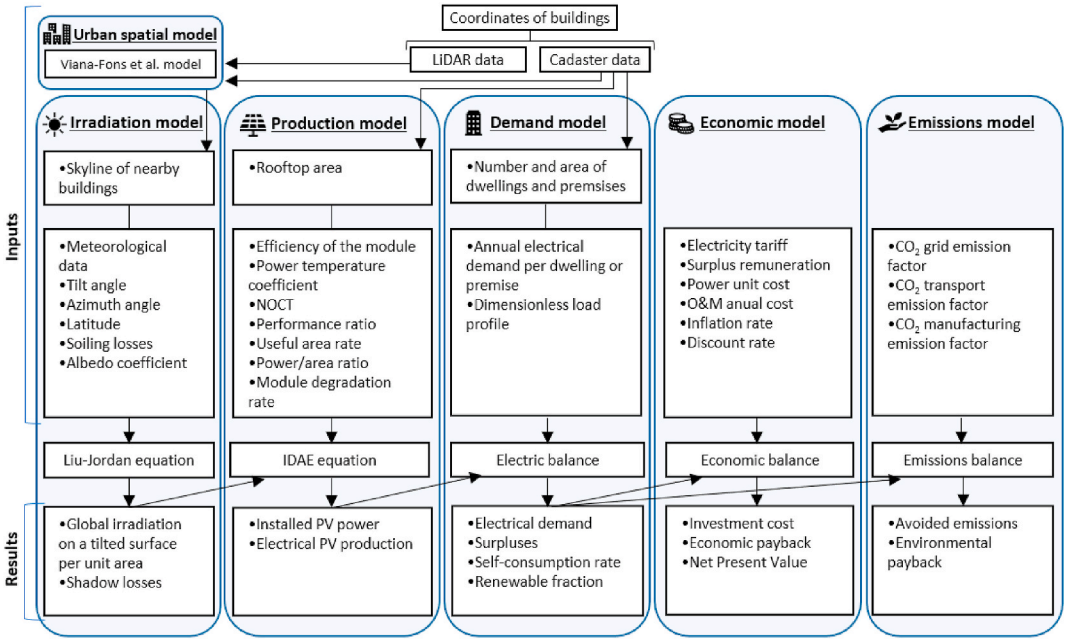

Fig. 2. Block diagram of the PV techno-economic model.

requires to scan the environment for each time step. In contrast, the second method only requires a single scan to obtain the skyline of nearby buildings. The calculation of the shadow losses is performed using sun maps or knowing the sun path. As a consequence, the global irradiation is based on a single representative point selected manually for each rooftop. The latter is chosen as the area with less shadows from nearby buildings, chimneys, parapets, elevator shafts, etc.

The skyline of the surrounding buildings is calculated given the coordinates of a representative point of the rooftop. This skyline is the first step to quantify the shadow loss factors for beam and diffuse irradiation. Both factors have been obtained by means of a GIS-based model, developed by Viana-Fons et al. [33], which employs the cadaster data as inputs. The cadaster data provides the geometry of the rooftops of the buildings, and the height of the buildings is obtained from LiDAR data [34]. As a result, each polygon is assigned a determined height, hereby creating a prismatic model. The assumed error for this prismatic approach is enough to accurately estimate the shadow losses in the rooftops of Valencia [35]. Additionally, according to Filip Biljecki et al. the potential improvement on the level of detail is very small [36].

The median of the Z coordinate of the LiDAR points contained in the building footprints has been used for the calculation of the height of the buildings in the vector-based 3D city model. The median is a high robust statistic estimator for this application according to Viana-Fons et al. [37]. Through geometric calculations proposed by Gál and Unger [38], the model generates a skyline profile. For each azimuthal angle step, set to 5°, the skyline is obtained within a radius of 200 m from the calculation point on the rooftop. According to the preliminary results reported by Chen et al. [39], considering obstacles located further than 300 m do not yield more accuracy to the SVF calculation.

2.2.2. Irradiation model

The isotropic radiation model from Liu and Jordan [40] has been employed in the model. For a given building rooftop, the program calculates the hourly global irradiation on the PV module. The azimuth angle considers the shadows cast by the surrounding buildings and nearby obstacles. The components of the horizontal irradiation have been previously obtained from the Typical Meteorological Year data of Valencia provided by EnergyPlus [41] and the equations of J.J. Michalsky [42] for the sun path, and the ground reflectance.

The shadow losses affect the beam and the diffuse components, respectively. They have been included in the calculation of the Shading Factor (SF) and the Sky View Factor (SVF).

Moreover, the skyline must contemplate those regions of the visible sky that are blocked by a given surface of the surroundings. For this purpose, the analytical expression proposed by Arbi Gharakhani et al. [43] is used to generate a profile which associates an elevation angle for each azimuth to the sky which is blocked by the panel. This obstacle profile is combined with the skyline of the surrounding buildings, resulting in a new combined obstacle skyline on which the shadow loss factors (SF and SVF) are calculated.

Additionally, soiling losses of 5% have been applied to the global irradiation, the result is denoted as effective global irradiance.

2.2.3. Production model

The hourly PV energy production is calculated according to the Spanish guidelines from IDAE [44]. The latter assume typical values of PR and an efficiency of the PV module, which depends on the temperature considering a standard power's temperature coefficient and a normal operating cell temperature (NOCT). The production is scaled considering the effective area of panels on the rooftop area. The total area is reduced by 30% to consider other space requirements such as for Heating Ventilation Air Conditioning), chimneys, or shadows from the surrounding walls. An annual degradation of the power of the modules of 5% has also been considered.

2.2.4. Demand model

The PV production is compared with the electricity demand curve of the entire building. The latter is generated assuming a dimensionless hourly demand profile [27] multiplied by the annual electricity demand of the building, considering all its dwellings and premises from the cadastral information. The model assumes a same profile of the load curve for all dwellings and other premises of the building.

2.2.5. Economic model

The economic calculations have been developed according to the self-consumption modality with surpluses under compensation of RD 244/2019 [45]. The latter allows the energy surpluses to be sold to the grid to perceive a reduction which is as maximum the monthly electricity bill with no PV. The electricity and compensation prices are obtained from time series of 2018 provided by the corporation which

operates the Spanish electric grid (Red Eléctrica de España, REE). The assumed investment costs depend on the installed power as indicated in Table 1. Additionally, a yearly operation and maintenance cost has been considered, as well as a yearly inflation rate and discount rate, as indicated further on in Table 2.

2.2.6. Emissions model

The model also estimates the avoided emissions due to savings from the electricity grid considering an emission factor, as well as the environmental impact in the manufacturing of PV modules and its transportation.

The emission factors, together with all the other inputs, are listed in Table 2. The model is calculated in hourly terms and the simulations are run throughout the entire life cycle of the facility (25 years).

3. Results and discussion

The correlations use as a starting point the performance of PV installations located in potential roof tops of Valencia. The performance is obtained with the techno-economic model described in section 2.2. In section 3.1, the techno-economic model is validated. In section 3.2, the performance results obtained with the model are employed for the development of the correlations.

3.1. Validation of the techno-economic model

The energy production results provided by the techno-economic model have been compared with the results provided by the software SAM. Both models have been executed for a same PV self-consumption facility, which is summarized in Table 3 and is located on a rooftop of a public building in Valencia (39.469072°, −0.340381°). Both models are fed with the same inputs and climate data. The Simple Module Efficiency Model was chosen in SAM and the shadow losses were introduced with the feature "solar azimuth-by-altitude beam irradiance shading losses", considering the skyline obtained with the Viana Fons et al. model [37]. Fig. 3 compares the PV production obtained with both models. The RMSE and mean absolute error (MAE) are 0.525 kWh and 0.233 kWh, respectively, and the deviation is of ± 10% except for low production levels at afternoon hours. This is probably due to the fact that the azimuth resolution allowed in SAM (20° each step) to introduce the skyline of surrounding obstacles is less accurate than the one obtained with the techno-economic model (5° each step). As a result, there are small deviations in radiation results in late hours when the sun is covered by a building in the west. Moreover, the PV production in the late afternoon may be below or above the inverter electrical thresholds defined in SAM. This aspect has not been considered in the techno-economic model to simplify the calculations.

3.2. Payback regression model

The payback regression model is obtained from the analysis of the simulation results provided by the techno-economic model. The first step is to define the minimum sample of buildings and to define the predictors.

Table 1
Unit power costs as a function of the installed power.

Power range, P (kW_p)	Power unit cost (€/kW_p)
$P \leq 10$	1.600
$10 \leq P \leq 20$	$1.800 - 20 \cdot P$
$20 \leq P \leq 50$	$1.566 - 8,33 \cdot P$
$50 \leq P \leq 500$	$1.178 - 0,556 \cdot P$
$P > 500$	900

Table 2
Summary table of all the inputs of the simulations.

Parameter	Value	Units	Source
Default module tilt angle	30	°	–
Default azimuth tilt angle	0	°	–
Latitude	39,4697	°	–
Soiling losses	5	%	M. R. Maghami et al. [46]
Albedo coefficient	0,2	–	P. Gilman et al. [47]
Efficiency of the module	15	%	Ó. Perpiñán [48]
Power temperature coefficient of the module	−0,4	%/°C	M. C. Brito et al. [49]
NOCT	45	°C	IDAE [44]
Performance ratio	0,8	–	W.G.J.H.M. van Sark et al. [50]
Useful area ratio	0,7	–	–
Area/power ratio	10	m^2/W_p	Grupotech [51]
Module degradation rate	2	%/year	D.C Jordan et al. [52]
Electrical demand per dwelling	3500	kWh/year	IDAE [53]
Electrical demand in commerces	300	kWh/m^2year	ANPIER [54]
Electrical demand in offices	137,75	kWh/m^2	Cámara de Madrid [55]
Electric tariff (mean)	0,12,335	€/kWh	REE [56]
Surplus remuneration	0,046,584	€/kWh	REE [57]
O&M costs	9,35	€/W_p	J.Chase [58]
Inflation rate	1,30	%	inflation.eu [59]
Discount rate	7	%	CNMC [60]
CO_2 grid emission factor	0,267,262	$kgCO_2$/kWh	REE [61]
CO_2 transport emission factor	0,151	$kgCO_2$/t·km	PVsyst [62]
CO_2 manufacturing emission factor	932	$kgCO_2$/kW_p	PVsyst [63]
Module weight/power ratio	0,07047	t/kW_p	Atersa [64]
Life cycle of the facility	25	years	M. S. Chowdhury et al. [63]

Table 3
Characteristics of the PV facility located in Valencia for the model validation.

Characteristic	Value	Units
Installed power	25.94	kW_p
Total area of panels	133.03	m^2
Temperature coefficient	−0.36	%/°C
Maximum power voltage	33.54	V_{dc}
Open circuit voltage	37.38	V_{oc}
Module efficiency	19.5	%
Inverter nominal power	25	kW
Inverter efficiency	98.3	%
Tilt angle	10	°
Azimuth angle	0	°
Modules per string in subarray	Subarray1:22 Subarray2:18	–
Modules parallel in subarray	Subarray1:2 Subarray2:2	–

3.2.1. Assumptions and required sample size

The payback regression model has been applied to a random sample of multi-storey buildings with flat rooftops in the urban nucleus of Valencia.

As exposed in section 2.2 and in Fig. 2, PV facilities are influenced by buildings due to three different features: (i) the skyline of the surrounding buildings, which is associated with the shadow losses; (ii) the available rooftop area related with the potential economy of scale and with the energy production; and (iii) the demand profile, which defines the amount of surpluses and the self-consumption levels. Given the previous variables, four different dimensionless predictor variables were initially tested to predict the economic payback:

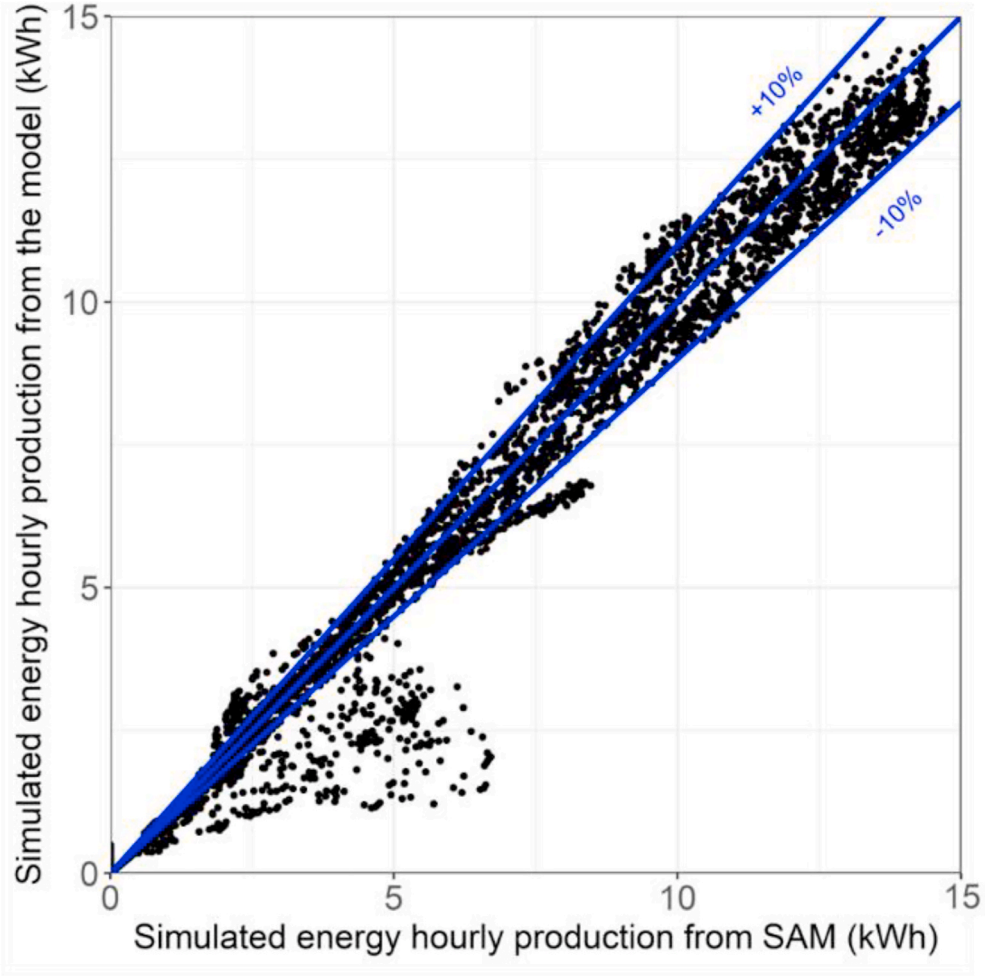

Fig. 3. Validation of the hourly PV production from the techno-economic model compared with the energy results obtained from SAM for a same facility in Valencia.

- The percentage of shadow losses (SL) defined as the ratio between the yearly global irradiation on the tilted surface including shadows and the yearly global irradiation on the tilted surface without shadows.
- The cost ratio (CR) defined as the relationship between the power unit cost of the facility and the maximum power unit cost (assumed as 1.6 €/W_p for small facilities, as shown in Table 1). This predictor indirectly considers the available rooftop area since it is related with the power unit costs and to the economy of scale.
- The building power ratio (BPR) defined as the relationship between the peak power of the demand curve and the peak PV installed power.
- The Surpluses Ratio (SR) understood as ratio between yearly energy surpluses (S_{PV}) and the production (E_{PV}). This ratio is important since surpluses in Spain are treated differently than self-consumption at an economical level.

The minimum required sample size is determined by means of an F-test performed with the software G*Power [65]. The latter carries out statistical power analyses, with the statistical F-test feature for MLR "Fixed model, R^2 deviation from zero" [66]. The F-test evaluates for a given sample size whether a continuous variable, the payback in this case, is significantly estimated by a set of predictors, in this case the SL, CR, BPR and SR. The program assumes as null hypothesis that the R^2 equals zero, and as alternative hypothesis that the R^2 is greater than zero, which means that there is a correlation between the predictors and the payback with a statistical significance.

In order to perform this test it is necessary to assign values to the type-I error, the power and the effect size index (f^2). The standard type-I and type-II errors have been fixed respectively as 5% and 20% (associated with a power of 80%, the probability of rejecting the null hypothesis). The latter values have been fixed taking as reference the five-eighty convention suggested by J. Cohen [67]. These values are also within the range proposed by other authors [68]. The effect size is set at $f^2 = 0.29$, which depends on the correlation coefficients between the four predictors and the payback. These correlation coefficients are obtained from the results of a sample of 200 buildings simulated prior to this test and yield similar values to the ones shown in Fig. 4.

As a result of the F-test, the minimum sample of buildings is 47 with a power of 80,91%. In other words, there is a probability of 80,91% that the R^2 will significantly be greater than zero if the sample is of 47 buildings or more. Nevertheless, in order to cover all the districts of the urban nucleus, at least 50 buildings per district have been selected, hereby yielding a total of 1035 buildings for the entire city shown in Fig. 4. This amount has been finally reduced to 893 buildings after filtering the paybacks which are higher than the facility useful life [63]. As discussed in section 3.3.1, the sample size decision is backed by analyzing the RMSE for several test and train ratios (the proportion of the dataset intended to fit the model and its complementary intended to validate the model).

3.2.2. Regression model

Due to the fact that the MLR assumes that the residuals of the model are distributed normally [69] the normality of the filtered payback dataset of 893 buildings has been assessed with a Shapiro-Wilk test. The null-hypothesis is that the economic payback is distributed normally,

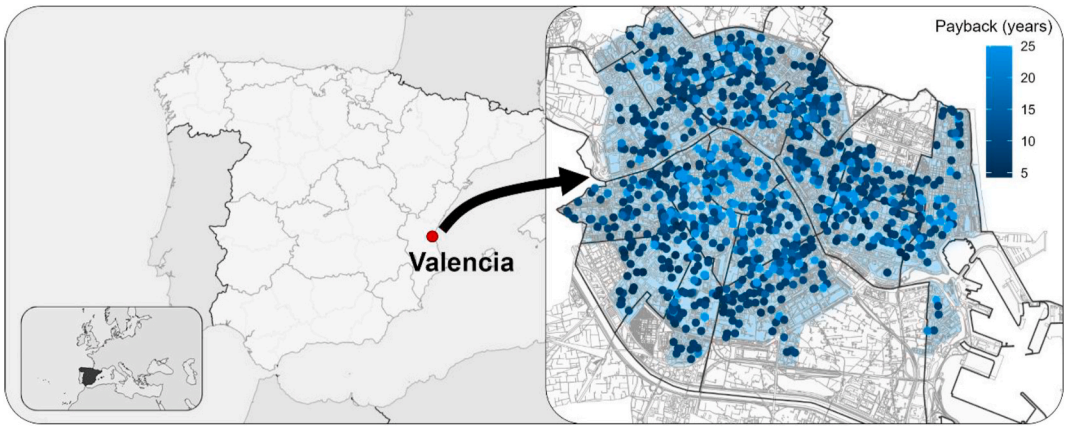

Fig. 4. Location of the simulated buildings in the city of Valencia, Spain.

consequently if the p-value is less than a type-I error of 5% [67], the null hypothesis is rejected. The test provides a p-value of $2.2{\cdot}10^{-16}$, thus the data does not meet a pure normality assuming a confidence level of 95%. Furthermore, the distribution is moderately right-skewed (skew = 1.23), which indicates an asymmetric density distribution with a long tail on the right side. in order to reduce its right skewness, the payback variable has been transformed with the inverse root square ($Payback^{-0.5}$), as suggested Tabachnick et al. [70]. A normal distribution has then been obtained with a p-value of 0.18 for the Shapiro-Wilk test and a with a distribution which is practically symmetric (skew = −0.03). Finally, the payback dataset has been randomly split using a 20:80 ratio, to create the training dataset and test dataset, respectively. The first one is used to train the MLR model and the second one to assess and validate the model.

Once the minimum sample size has been obtained and the payback has been fitted properly, the correlation matrix of Fig. 5 helps to obtain a preliminary assessment of the four predictors given their impact on the predicted variable, which is the economic payback.

As a first step it is necessary to reduce the multicollinearity among predictors. Fig. 5 shows a strong positive correlation of 0.89 between the predictors BPR and SR, while the correlation values among the other predictors are negligible.

For this reason, a polynomial regression of degree six has been introduced to reflect the relationship between the SR and the BPR (as denoted by SR* in Equation (1)). As a result, the MLR model presented in Eq. (2) predicts the economic payback with only three features (SL, CR and SR), as also shown in Fig. 6. From the first row of this correlation matrix, the degree of influence of each predictor is determined. SL has the biggest impact, followed by the CR, and finally SR* in a lower level.

$$SR^{*}=\frac{S_{PV}}{E_{PV}}=k_0+k_1{\cdot}BPR+k_2{\cdot}BPR^2+k_3{\cdot}BPR^3+k_4{\cdot}BPR^4+k_5{\cdot}BPR^5+k_6{\cdot}BPR^6 \tag{1}$$

Finally, the MLR for the payback is described in equation (2). The regression parameters are estimated by ordinary least squares.

$$\frac{1}{\sqrt{PB}}=k_0+k_1{\cdot}SR^{*}+k_2{\cdot}CR+k_3{\cdot}SL+k_4{\cdot}SL^2 \tag{2}$$

The coefficient results for both regressions are gathered in Table 4. The correlations are very good given the high R^2 values. The negative sign of the coefficients shows that an increase of any of the predictors implies an increase of the payback. Considering their absolute value and the correlation matrix, the most important predictor is CR, followed by SL and finally, to a lower extent, SR*.

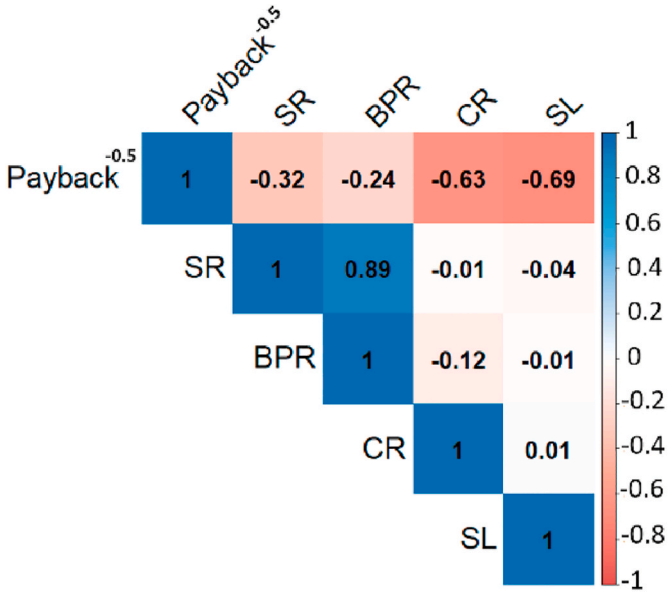

Fig. 5. Correlation matrix with the preliminary predictors.

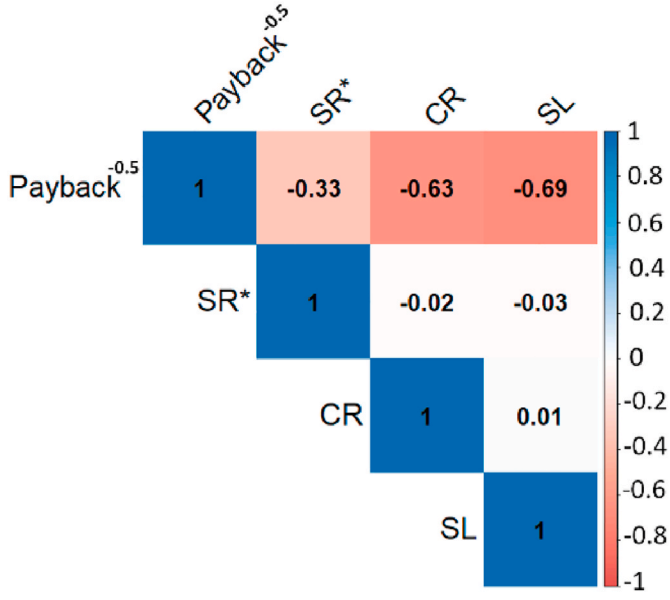

Fig. 6. Correlation matrix with the final predictors.

Table 4
Coefficients of the polynomial regression (Equation (1)) and the MLR model (Equation (2)).

Regression	k_0	k_1	k_2	k_3	k_4	k_5	k_6	R^2
$SR^* = S_{PV}/E_{PV}$	0.036	2.107	0.822	−0.612	−0.026	0.251	−0.110	0.9975
$1/\sqrt{PB}$	0.586	−0.209	−0.279	−0.234	−0.223	–	–	0.9951

3.3. Validation of the regression model

The previous models have been fed with the test dataset, and the predicted values have been compared with the ones from the complex model. According to Fig. 7, 97.97% of the predicted values present a relative error lower than 5%, and there are only three outliers in total. The MLR tends to over-predict slightly the payback in general, whereas the predictions with the greater residuals are underpredicted.

The errors shown in Table 5 indicate that the model provides accurate payback values, as illustrated by the RMSE which is of only 0.48 years. This value is completely assumable since the purpose of this regression is to provide an order of magnitude for energy planning.

3.3.1. Analysis of the errors depending on the test/training data ratio

An analysis of the error dispersion depending on the training set size has been carried out to demonstrate that the chosen sample size is robust and to guarantee an accurate evaluation error score independent of the training and test data partition. For this purpose, the training dataset size is increased from 100 to 700 by steps of 100. For each step, the original dataset is split into a random training sample and its complementary for testing is taken. Finally, the RMSE and MAE are calculated by repeating the process 1000 times, resulting in a different error value in each repetition due to the randomness of the sampling. The error distributions for each training dataset size are reflected in Fig. 8 and Fig. 9. The mean values of the RMSE and MAE register a very slight reduction, hereby confirming that a sample size of 200 buildings for train data is large enough to present an accurate regression. In both figures, there is a slight increase of the error between the 400 and 500 samples due to an overfitting of the model. The model reproduces too closely a particular dataset for samples larger than 400 buildings, consequently leading to poor generalization when predicting new testing data.

Additionally, an independent 10-fold cross-validation of the MLR model has been carried out. This is important to contrast the previous errors with a standardized methodology which is generally employed to validate regression models. The payback dataset is randomly split with a 20:80 ratio into 10 distinct subsets called folds. Afterwards, the MLR model has been fitted 10 times, choosing every evaluation step a different fold to train it and selecting the complementary folds to test it with the payback results from the complex techno-economic model. The results are similar to the previous plots in Figs. 8 and 9 with an average RMSE of 0.59 years and a MAE of 0.28, as well as a standard deviation of 0.043 and 0.008 years, respectively.

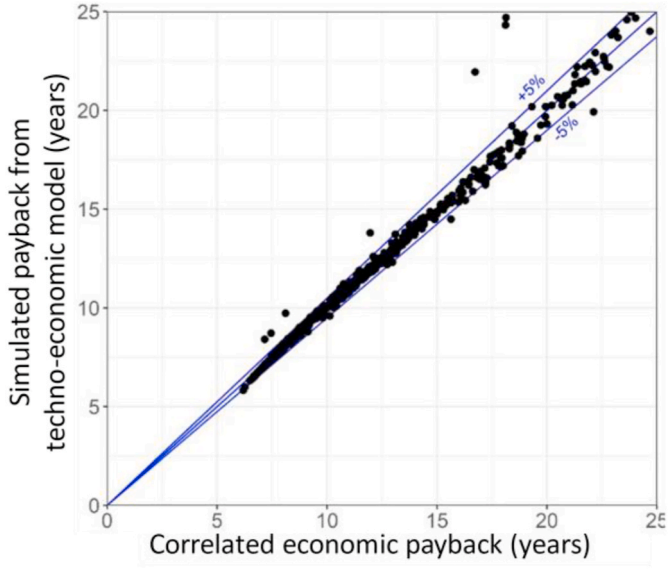

Fig. 7. Results and validation of the MLR model to predict the payback.

Table 5
Errors provided by the polynomial regression to estimate SR and the MLR to estimate the PB.

Regression	RMSE	MAE	Units
$SR^* = S_{PV}/E_{PV}$	0.00398	0.00306	–
$1/\sqrt{PB}$	0.48242	0.19189	years

3.3.2. Regression results for other locations

In order to ensure the replicability of the methodology for other locations, two regressions have been proposed, which combined estimate the yearly PV energy production, a value that can be easily converted into economic savings.

The first regression consists of a MLR model to estimate the yearly PV production in Valencia, depending on the installed peak power (P_{PV}) and SL.

$$E_{PV,\ building,\ Valencia}(P_{PV}, SL) = k_0 + k_1 \cdot P_{PV} + k_2 \cdot SL + k_3 \cdot P_{PV} \cdot SL \quad (3)$$

The production results obtained with the previous Eq. (3) for the sample of buildings described in section 3.2.1 have been compared in Fig. 10 with the results of the techno-economic model, obtaining an RMSE of 91.91967 kWh/year and a relative error lower than 5% in all cases

The second correlation is the simple linear regression shown in equation (4), which has been introduced to adapt the PV production (with SL = 0%) from the previous MLR model to the climatic conditions of any given location. This conversion only depends on location data such as the yearly global horizontal irradiation ($G_{0,\ location}$) and the mean ambient temperature ($T_{location}$).

$$E_{PV,location}\left(G_{0,\ location},\ T_{location}\right) = k_0 + k_1 \cdot G_{0,\ location} + k_2 \cdot T_{location} \quad (4)$$

The combination of both regressions enables the calculation of the yearly PV production from any given location, as indicated in equation (5). Fig. 11 presents the validation results for several locations for facilities with null shadow losses. The deviation is below 5% for 12 of the 15 locations assessed and the regression model tends to slightly overpredict the yearly production, except for the high latitudes.

$$E_{PV,building,location} = E_{PV,\ building,\ Valencia}(P_{PV}, SL) \cdot \frac{E_{PV,location}\left(G_{0,\ location},\ T_{location}\right)}{E_{PV,location}\left(G_{0,\ Valencia},\ T_{Valencia}\right)} \quad (5)$$

Additionally, shadow losses in the range from 0 to 40% have been simulated in different locations to check that there is still a linear relationship between $E_{PV,\ Location}$, $G_{0,\ location}$, and $T_{location}$. Fig. 12 shows these results, revealing that most of the points are within a deviation of ±

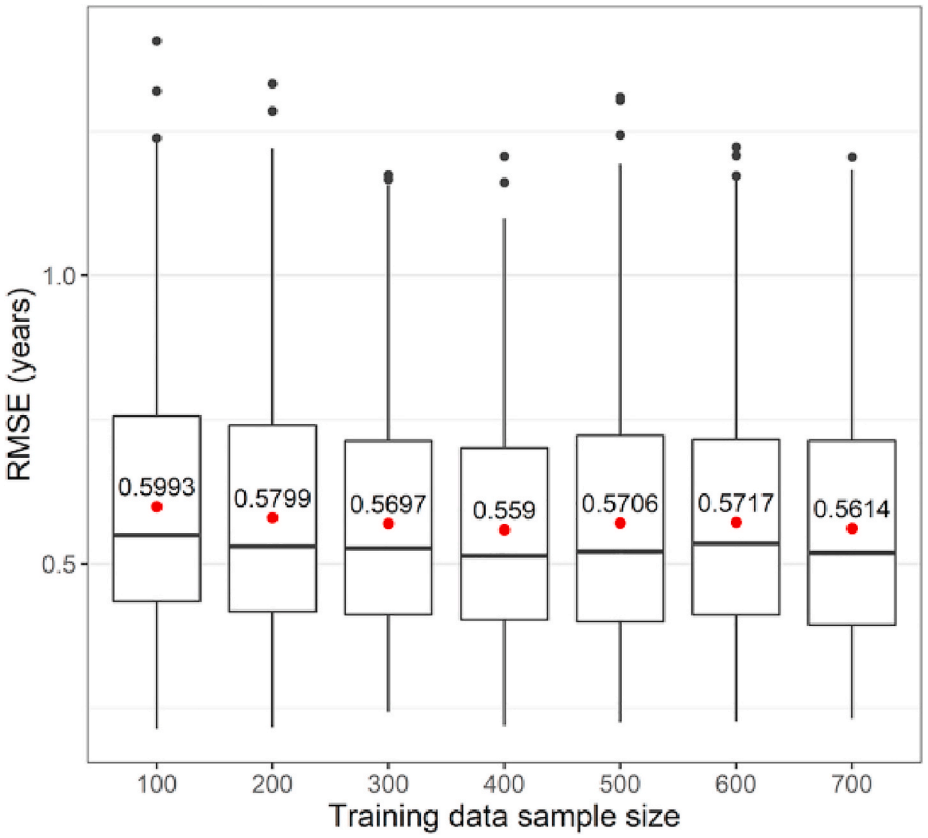

Fig. 8. RMSE boxplots for different train/test splits.

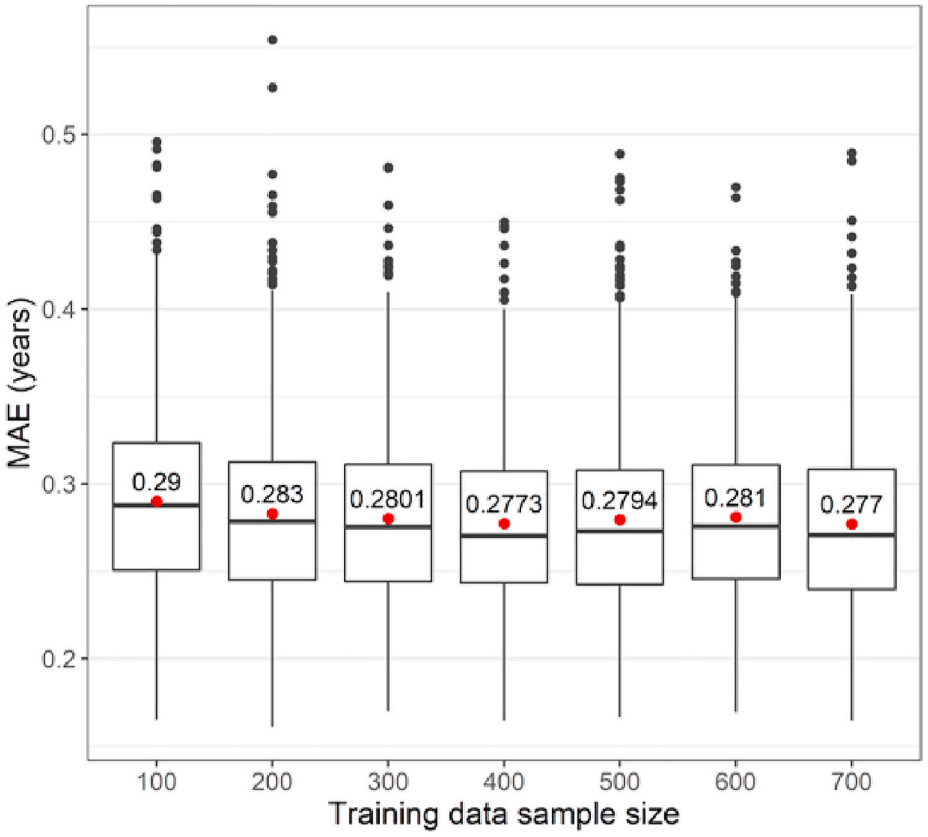

Fig. 9. MAE for different train/test splits.

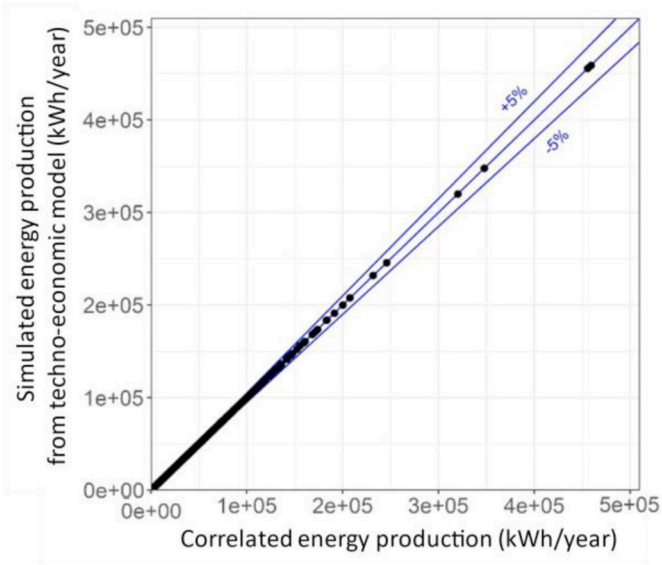

Fig. 10. Results and validation of the MLR model to predict the energy production.

10%. In general, there is an underprediction when the shadow losses increase for a same location. Again, as described in Fig. 11, there is an underprediction in Brussels (the location in Fig. 11 with a highest latitude), however for regular shadows and latitudes the regression model provides accurate results providing a RMSE of 3.20 kWh/kW$_p$·year.

Finally, the coefficients and errors of Equations (3)–(5) are gathered in Table 6.

The previous regressions can be employed as a starting point to make the balance with the electrical demand, to apply other costs or electricity prices and to calculate the surplus remuneration according to appropriate climate and regulation (net-metering, feed-in-tariff, and other schemes gathered by Campos Inês et al. [30]).

3.4. Overall analysis of the assessed multi-storey buildings

The main results obtained with the techno-economic model for the sample of 893 buildings (those whose payback is under 25 years) are showcased in the boxplots of Fig. 13, Fig. 14 and Table 7.

According to Fig. 13, the average economic payback for the sample is 11.59 years. 40.42% of the total results yield paybacks between 8 and 11 years and only 0.33% provide values under 6 years. As mentioned in section 3.2.2, the economic payback distribution is right skewed since there is a wide dispersion of cases for which the profitability is hindered by shadows and/or a low match between production and demand or high costs. In fact, this tail of the distribution would be larger if the discarded facilities with paybacks beyond the lifecycle had been represented (13.72% of the original dataset).

The environmental payback, understood as the time to recover the emissions generated during the manufacturing and transport of the panels, presents an average of 2.31 years, which shows a high positive impact on the environment even on a short term. The low standard deviation is due to the assumption of a similar emission factor for all the cases. The dispersion could increase if different manufacturers had been considered. However, this analysis provides an order of magnitude of the notorious difference between the economic and environmental paybacks.

As Fig. 14 shows, the low levels of exports, with an average of 3.62% of the yearly production, are explained by the high level of electricity demand in comparison with the PV production, which is limited by the effective rooftop area. These small exportation values together with the low prices of surplus remuneration are the main reasons why electricity export does not play an important role to improve the economic payback for these buildings. The same conclusions were obtained with the MLR model. Given the reduced exportation, practically for half of the simulated buildings the energy generated is self-consumed on site.

Regarding the renewable fraction shown in Figs. 14 and 17.73% of the total grid electricity consumption could be supplied entirely with on-site PV production. The highest renewable fraction and exportation ratesare achieved in buildings with a yearly PV production higher than 65% of the yearly demand. In general, these installations are oversized.

The shadow losses usually have low values for this type of building due to their elevated height. An average shadow loss of 17.73% is

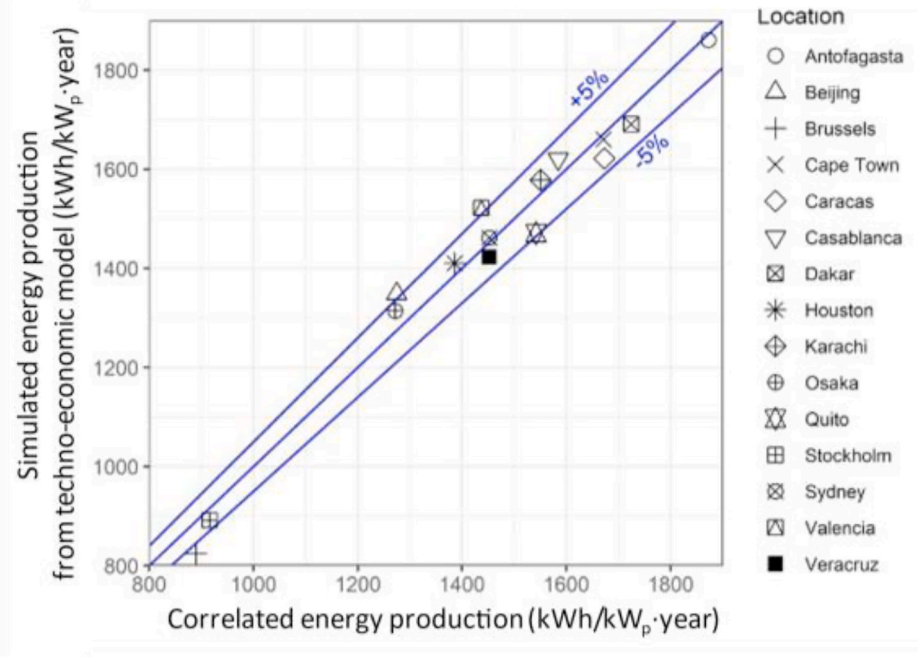

Fig. 11. Results and validation of the polynomial regression model to predict the SR.

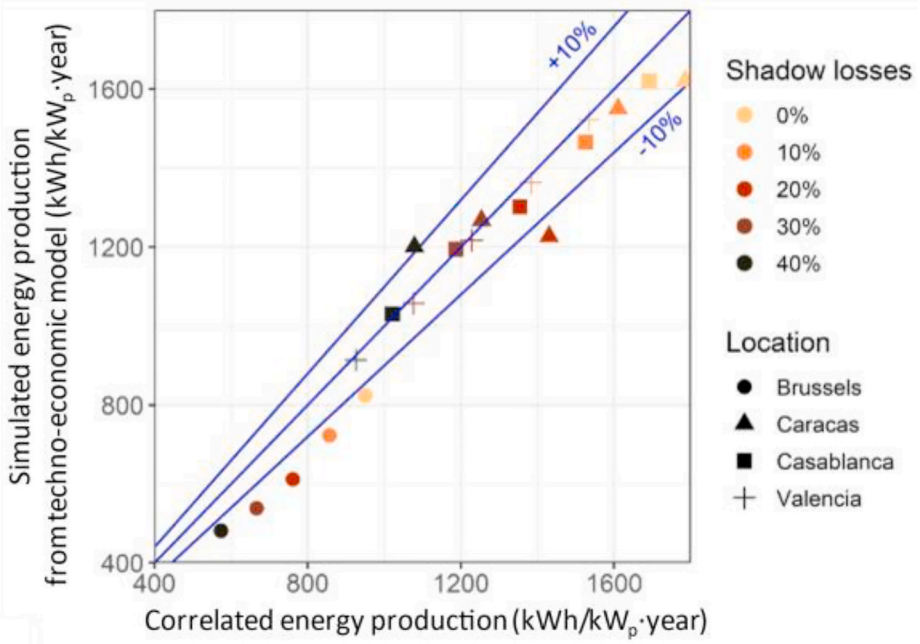

Fig. 12. Results and validation of the MLR model to predict the payback.

Table 6
Coefficients of equations (3)–(5).

Regression	k_0	k_1	k_2	k_3	RMSE (kWh/kW$_p$ year)	MBE (kWh/kW$_p$ year)	R^2
$E_{PV,\ building,\ Valencia}(P_{PV}, SL)$	−13.167	1534.410	−85.760	−1510.610	2.116	0.148	0.999
$E_{PV,location}(G_{0,\ location},\ T_{location})$	185.705	0.841	−6.499	–	3.200	2.751	0.970
$E_{PV,building,location}$	–	–	–	–	3.200	2.751	0.970

obtained and the latter drops significantly down to 10.39% if the median is considered. These losses are generally due to shadows cast by the railings, elevator shafts and chimneys. In most modern districts, thanks to urban planning, most of the buildings have a similar height and consequently they hardly produce shadows between them. This phenomenon can be noticed with the spatial distribution of paybacks shown in Fig. 4, where downtown buildings present higher paybacks due to abrupt skylines, whereas the modern districts on the outskirts yield lower paybacks.

At a more detailed level in the building characterization, the buildings which present the best profitability results share the following characteristics:

- Large rooftop areas, which imply lower unit costs due to the economy of scale.
- High levels of electricity consumption, since the PV generation is intended to reduce the costs of the energy term of the electricity bill, whose cost is higher than the current surplus remuneration.
- Low percentage of shadow losses to maximize the PV production.
- Coincidence of consumption hours with radiation hours to maximize the energy and bill savings and reduce surpluses, which provide a lower income.

The above-mentioned characteristics generally fit with the characteristics of industrial buildings and residential multi-storey buildings. Both typologies are consequently the most suitable for PV production. Taking the above-mentioned characteristics into account, an alternative to subsidies that could help to improve the payback consists of creating energy communities with a same PV facility, but aggregating the electrical demand from several buildings. As a result, all of the produced energy could be self-consumed and the savings in the electric bill would be higher.

According to the techno-economic model, PV facilities in single-family houses do not present as favorable economic results as multi-storey buildings, although they present a greater renewable fraction (with an average of 30% of the PV production) and exportation rates (with an average of 40% of the production), as confirmed by simulating 100 houses. The average of their shadow losses registered is 35%, which contrasts with the average of 10% for multi-storey buildings.

Likewise, with the results of the sample of buildings, Fig. 15 shows a gradient plot representing the influence of the two main predictors (SL, and power unit costs) on the economic payback. A greater weight of the unit power cost is appreciated. For costs above 1.5 €/W$_p$, the shadow losses must remain lower than 40% to guarantee a payback lower than the facility life cycle. The gradient plot has been constructed by means of a linear interpolation of the discrete points of the sample in a 200 × 200 grid. The presence of outliers and their consequent discontinuities in the plot for costs over 1.4 €/W$_p$ are because the selected predictors do not explain entirely the payback for these specific points.

4. Conclusions

The present work has been developed to shorten the gap between energy planners and detailed simulation models of PV facilities. A MLR model has been developed, in a similar approach as recent studies from literature, although including the main novelty of addressing the economic impact and ensuring a high replicability since it can be applied for other locations. As an application, the mentioned methodology has been applied for the most common buildings in the city of Valencia, which are multi-storey residential buildings.

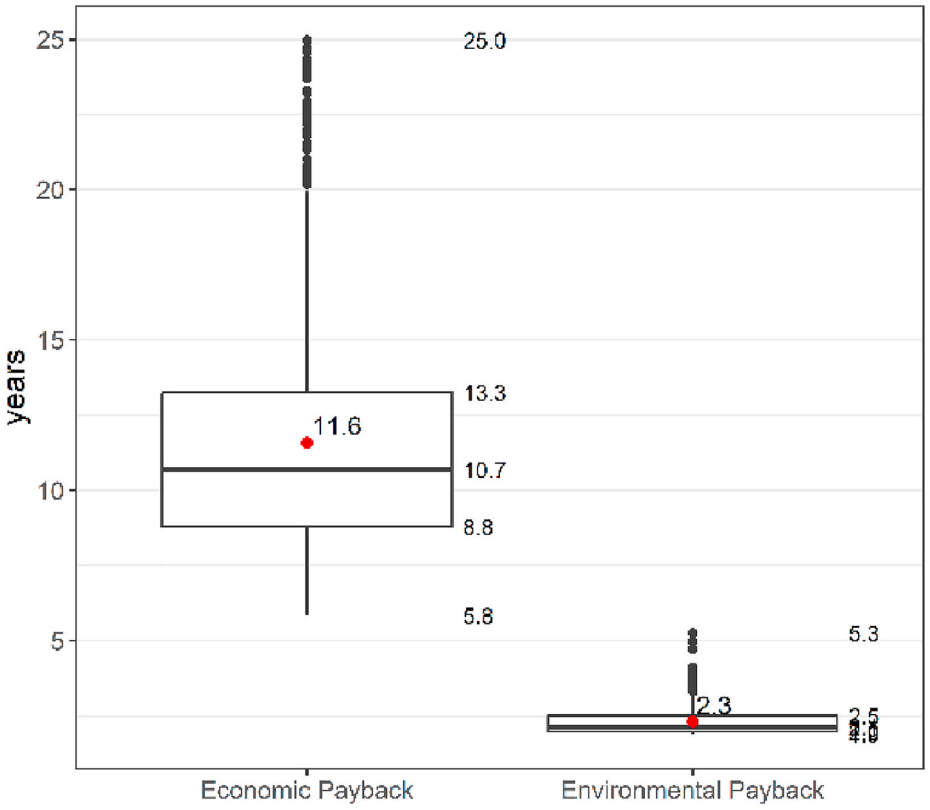

Fig. 13. Economic and environmental payback results for the sample of buildings of Valencia.

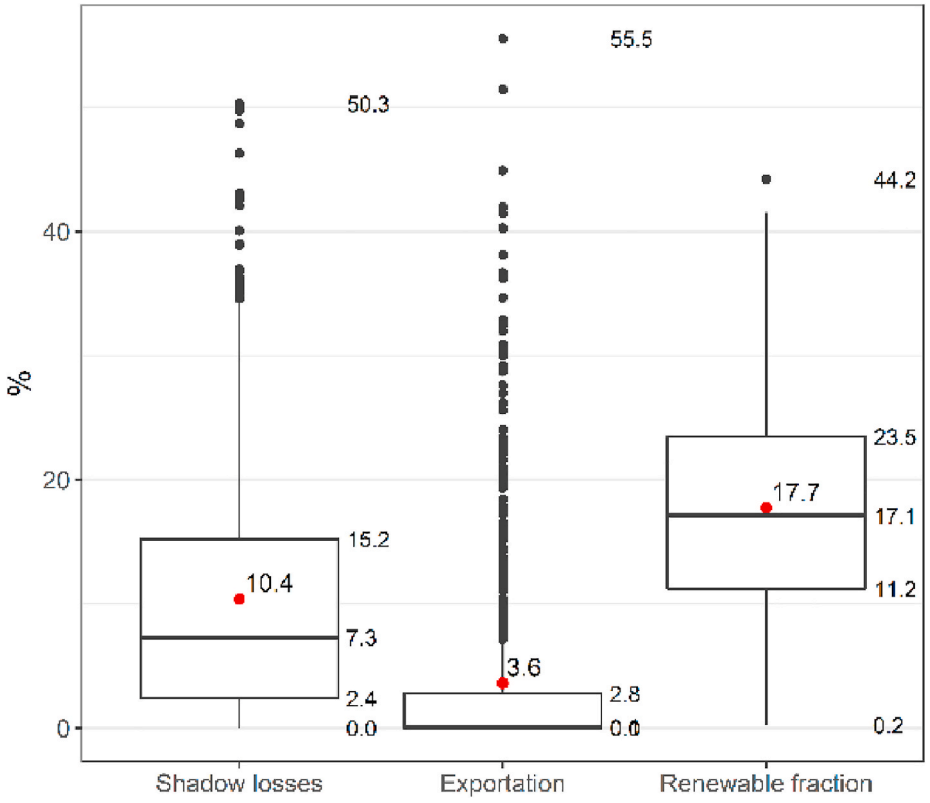

Fig. 14. Shadow losses, exportation ratio and renewable fraction for the sample of buildings of Valencia.

Table 7
Statistical results for the sample of buildings in Valencia.

Variable	Units	Mean	Standard deviation	Skewness[a]	Minimum	Q1	Median	Q3	Maximum
Economic Payback	years	11.59	3.93	1.26	5.83	8.79	10.68	13.26	24.97
Environmental Payback	years	2.31	0.48	1.85	1.88	1.97	2.14	2.50	5.25
Shadow losses	%	10.39	10.15	1.29	0.00	2.40	7.31	15.21	50.28
Exportation	%	3.62	7.92	2.99	0.00	0.00	0.06	2.78	55.53
Renewable fraction	%	17.73	8.94	0.32	0.24	11.21	17.09	23.48	44.20

[a] Adimensional value.

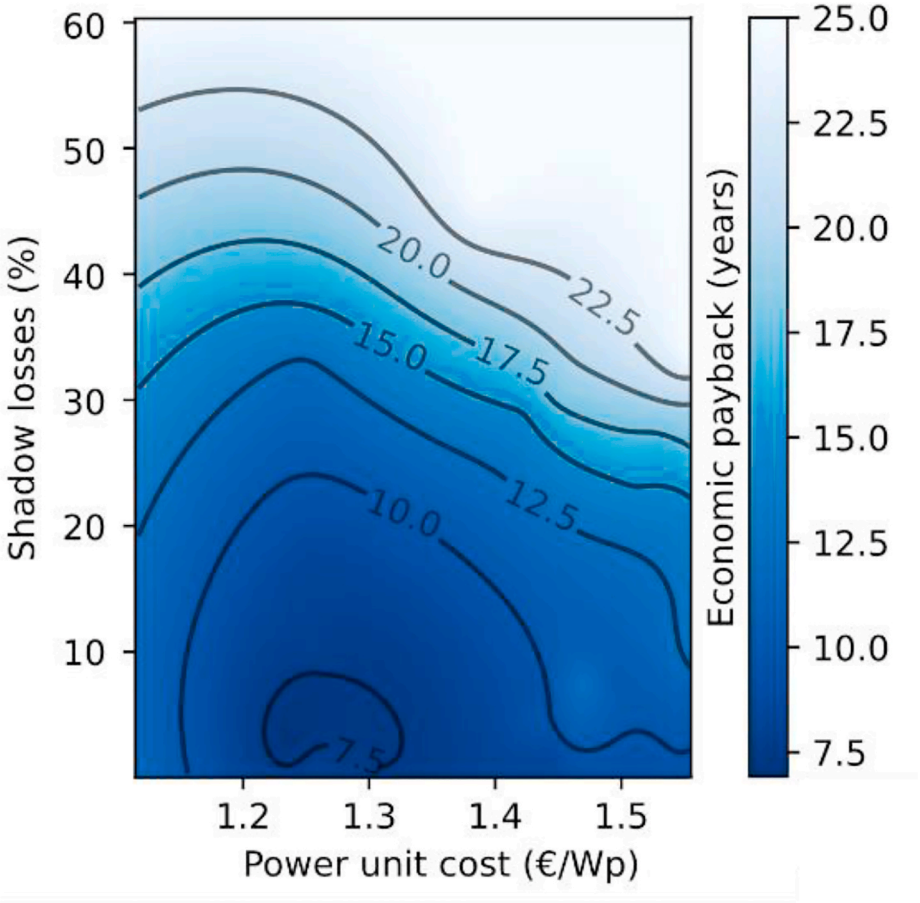

Fig. 15. Relationship between the economic payback and the most influential predictors: shadow losses and power unit costs for the sample of buildings of Valencia.

The MLR model is based on the results given by a complex techno-economic model, which has previously been compared and validated with SAM providing a RMSE of 0.53 kWh in the hourly PV production. The proposed MLR model has been validated by means of a cross-validation methodology which has provided a RMSE of 0.48 years which is perfectly assumable for energy planning purposes. As a complement for other countries, a combination of regressions has been proposed to estimate the PV production on any rooftop given the capacity, shadow losses and climatic data. The relative errors for this methodology are close to 10% for the studied locations with a R^2 value of 0.97.

The following conclusions have been obtained when applying the methodology to the residential multi-storey buildings of Valencia:

- The key drivers on the payback are the shadow losses and the economy of scale. The best economic paybacks are obtained in large available rooftop areas.
- On the demand side, buildings with high levels of electricity demand tend to profit in a high percentage from on-site energy generated from self-consumption. The surpluses are very low and all the PV production is translated into energy and bill savings. In the case of low consumption levels such as buildings with very few dwellings, the savings are very limited, therefore their cashflows are low in comparison with the investment costs.
- For high electricity demands, the sale of surpluses does not represent a relevant factor to generate large savings and reduce the payback. The sale price in Spain is lower than the price of the bill. One solution to reduce the high paybacks in single-family houses and buildings with low energy demand can be the promotion of energy communities, since the results show that adding consumption and reducing exports leads to a better profitability. As future work, the authors will analyze in more detail the opportunities of PV production in energy communities.

Credit author statement

By means of the present document, and as corresponding author of our work, I declare which was the detailed contribution of each of the

different authors:**Enrique Fuster-Palop**: Methodology, Software, Validation, Investigation, Writing - Original Draft. **Carlos Prades-Gil**: Resources, Investigation, Supervision, Funding acquisition. **X. Masip**: Resources, Investigation, Supervision, Funding acquisition. **Joan D. Viana-Fons**: Resources, Investigation, Software. **Jorge Payá**: Conceptualization, Writing - Review & Editing, Supervision.

Declaration of competing interest

The authors declare that they have no known competing financial interests or personal relationships that could have appeared to influence the work reported in this paper.

Acknowledgements

This study was developed owing to the support provided by the Chair of Urban Energy Transition of the Universitat Politècnica de València and the foundation Las Naves.

Additionally, this work was supported by The Energy Office of Valencia and the Statistics Office of the Valencia City Council, who collaborated by providing the data of the PV facility for the validation and their recommendations on the statistical analysis.

References

[1] EUROSTAT, "eurostat - data explorer. Complete energy balances." .
[2] EUROSTAT, "Eurostat - data Explorer. Supply, transformation and consumption of electricity." .
[3] IDAE, Estudios. Informes y estadísticas. IDAE; 2017.
[4] IEA. Electricity – world energy outlook. 2019. 2019.
[5] Gomez-Exposito A, Arcos-Vargas A, Gutierrez-Garcia F. On the potential contribution of rooftop PV to a sustainable electricity mix: the case of Spain. Renew Sustain Energy Rev 2020;132:110074. https://doi.org/10.1016/j.rser.2020.110074. Oct.
[6] IRENA. Solar PV module costs 2010-2018. 2019.
[7] Castellanos S, Sunter DA, Kammen DM. Rooftop solar photovoltaic potential in cities: how scalable are assessment approaches? Environ Res Lett 2017;12(12):125005. https://doi.org/10.1088/1748-9326/aa7857.
[8] Lobaccaro G, et al. A cross-country perspective on solar energy in urban planning: lessons learned from international case studies. Renew Sustain Energy Rev 2019;108:209–37. https://doi.org/10.1016/j.rser.2019.03.041.
[9] Pieter Gagnon RM, Jennifer Melius CP, Elmore R. Rooftop solar photovoltaic technical potential in the United States: a detailed assessment. 2016.
[10] Ngar-Yin Mah D, Wang G, Lo K, Leung MKH, Hills P, Lo AY. Barriers and policy enablers for solar photovoltaics (PV) in cities: perspectives of potential adopters in Hong Kong. 2018. https://doi.org/10.1016/j.rser.2018.04.041.
[11] Ordóñez J, Jadraque E, Alegre J, Martínez G. Analysis of the photovoltaic solar energy capacity of residential rooftops in Andalusia (Spain). Renew Sustain Energy Rev 2010;14(7):2122–30. https://doi.org/10.1016/j.rser.2010.01.001.
[12] Brito MC, Freitas S, Guimarães S, Catita C, Redweik P. The importance of facades for the solar PV potential of a Mediterranean city using LiDAR data. Renew Energy 2017;111:85–94. https://doi.org/10.1016/j.renene.2017.03.085.
[13] Freitas S, Catita C, Redweik P, Brito MC. Modelling solar potential in the urban environment: state-of-the-art review. Renewable and sustainable energy reviews, vol. 41. Elsevier Ltd; 2015. p. 915–31. https://doi.org/10.1016/j.rser.2014.08.060.
[14] Schallenberg-Rodríguez J. Photovoltaic techno-economical potential on roofs in regions and islands: the case of the Canary Islands. Methodological review and methodology proposal. Renew Sustain Energy Rev Apr-2013;20:219–39. https://doi.org/10.1016/j.rser.2012.11.078.
[15] Quesada B, Sánchez C, Cañada J, Royo R, Payá J. Experimental results and simulation with TRNSYS of a 7.2kWp grid-connected photovoltaic system. Appl Energy 2011;88(5):1772–83. https://doi.org/10.1016/j.apenergy.2010.12.011.
[16] Pedrero J, "IOP Conference Series. Earth and Environmental Science Assessment of urban-scale potential for solar PV generation and consumption. 2019. https://doi.org/10.1088/1755-1315/323/1/012066.
[17] Análisis CY, Caamaño Martín E, Díaz-Palacios Sisternes S. Potential solar fotovoltaico de las cubiertas edificatorias de la ciudad de Vitoria-Gasteiz: caracterización y análisis. 2017.
[18] Mangiante MJ, et al. "Economic and technical assessment of rooftop solar photovoltaic potential in Brownsville, Texas, U.S.A," *Comput*. Environ. Urban Syst. 2020;80:101450. https://doi.org/10.1016/j.compenvurbsys.2019.101450.
[19] Shirazi AM, Zomorodian ZS, Tahsildoost M. Techno-economic BIPV evaluation method in urban areas. Renew Energy Dec. 2019;143:1235–46. https://doi.org/10.1016/j.renene.2019.05.105.
[20] Omar MA, Mahmoud MM. Grid connected PV- home systems in Palestine: A review on technical performance, effects and economic feasibility. Renewable and sustainable energy reviews, vol. 82. Elsevier Ltd; 2018. p. 2490–7. https://doi.org/10.1016/j.rser.2017.09.008.
[21] Martín-Pomares L, Martínez D, Polo J, Perez-Astudillo D, Bachour D, Sanfilippo A. Analysis of the long-term solar potential for electricity generation in Qatar. Renewable and sustainable energy reviews, vol. 73. Elsevier Ltd; 2017. p. 1231–46. https://doi.org/10.1016/j.rser.2017.01.125.
[22] Trigo-Gonzalez M, et al. Development and comparison of PV production estimation models for mc-Si technologies in Chile and Spain. J Clean Prod 2021;281:125360. https://doi.org/10.1016/j.jclepro.2020.125360.
[23] Antonopoulos I, et al. Artificial intelligence and machine learning approaches to energy demand-side response: A systematic review. Renewable and sustainable energy reviews, vol. 130. Elsevier Ltd; 2020. https://doi.org/10.1016/j.rser.2020.109899.
[24] Calcabrini A, Ziar H, Isabella O, Zeman M. A simplified skyline-based method for estimating the annual solar energy potential in urban environments. Nat. Energy 2019;4(3):206–15. https://doi.org/10.1038/s41560-018-0318-6.
[25] Chatzipoulka C, Compagnon R, Kaempf J, Nikolopoulou M. Sky view factor as predictor of solar availability on building façades. Sol Energy Aug. 2018;170:1026–38. https://doi.org/10.1016/j.solener.2018.06.028.
[26] Poon KH, Kämpf JH, Tay SER, Wong NH, Reindl TG. Parametric study of URBAN morphology on building solar energy potential in Singapore context. Urban Clim Sep. 2020;33:100624. https://doi.org/10.1016/j.uclim.2020.100624.
[27] Trigo-González M, et al. Hourly PV production estimation by means of an exportable multiple linear regression model. Renew Energy May 2019;135:303–12. https://doi.org/10.1016/j.renene.2018.12.014.
[28] Müller J, Trutnevyte E. Spatial projections of solar PV installations at subnational level: Accuracy testing of regression models. Appl Energy 2020;265. https://doi.org/10.1016/j.apenergy.2020.114747.
[29] National Renewable Energy Laboratory, "Home - System Advisor model (SAM)." .
[30] Inês C, Guilherme PL, Esther MG, Swantje G, Stephen H, Lars H. Regulatory challenges and opportunities for collective renewable energy prosumers in the EU. Energy Pol 2020;138:111212. https://doi.org/10.1016/j.enpol.2019.111212.
[31] Lang T, Ammann D, Girod B. Profitability in absence of subsidies: A techno-economic analysis of rooftop photovoltaic self-consumption in residential and commercial buildings. Renew Energy Mar. 2016;87:77–87. https://doi.org/10.1016/j.renene.2015.09.059.
[32] Fuster E, Prades-Gil C, Masip X, Viana-Fons J, Paya-Herrero J. Evaluation of the solar photovoltaic generation potential of a district in the city of Valencia. SDEWES 2020:1–14. 2020.
[33] Viana-Fons JD, Gonzálvez-Maciá J, Payá J. Development and validation in a 2D-GIS environment of a 3D shadow cast vector-based model on arbitrarily orientated and tilted surfaces. Energy Build 2020:110258. https://doi.org/10.1016/j.enbuild.2020.110258.
[34] Centro Nacional de Información Geográfica, "Centro de Descargas del CNIG." .
[35] Viana-Fons JD, Gonzálvez-Maciá J, Payá J. Methodology for the calculation of the shadow factor on roofs and facades of buildings in urban areas. In: XI Congreso Nacional y II Internacional de Ingeniería Termodinámica (11-CNIT); 2019. p. 870–7.
[36] Biljecki F, Ledoux H, Stoter J. Does a finer level of detail of a 3D city model bring an improvement for estimating shadows? Lect. Notes Geoinf. Cartogr. 2017:31–47. https://doi.org/10.1007/978-3-319-25691-7_2. 9783319256894.
[37] Viana-Fons JD, Gonzálvez-Maciá J, Payá J. Development and validation in a 2D-GIS environment of a 3D shadow cast vector-based model on arbitrarily orientated and tilted surfaces. Energy Build 2020;224:110258. https://doi.org/10.1016/j.enbuild.2020.110258.
[38] Gál T, Unger J. A new software tool for SVF calculations using building and tree-crown databases. Urban Clim. 2014;10(P3):594–606. https://doi.org/10.1016/j.uclim.2014.05.004.
[39] L. Chen et al., "Sky view factor analysis of street canyons and its implications for daytime intra-urban air temperature differentials in high-rise, high-density urban areas of Hong Kong: a GIS-based simulation approach," Int J Climatol, vol. 32, no. 1, pp. 121–136.
[40] Loutzenhiser PG, Manz H, Felsmann C, Strachan PA, Frank T, Maxwell GM. Empirical validation of models to compute solar irradiance on inclined surfaces for building energy simulation. Sol Energy Feb. 2007;81(2):254–67. https://doi.org/10.1016/j.solener.2006.03.009.
[41] EnergyPlus, "Weather data by location | EnergyPlus," weather data download - Valencia 082840 (IWEC). .
[42] Michalsky JJ. "The Astronomical Almanac's algorithm for approximate solar position (1950-2050). Sol Energy 1988;40(3):227–35. https://doi.org/10.1016/0038-092X(88)90045-X.
[43] Rehman NU, Uzair M. The proper interpretation of analytical sky view factors for isotropic diffuse solar irradiance on tilted planes. J Renew Sustain Energy 2017;9(5). https://doi.org/10.1063/1.4993069. Sep.
[44] IDAE, "Pliego de Condiciones Técnicas de Instalaciones. Conectadas a red.". 2011.
[45] MTE "RD. 244/2019 Regulacion condiciones técnicas, administrativas y económicas del autoonsumo de energía eléctrica. 2019. p. 35674–719.
[46] Maghami MR, Hizam H, Gomes C, Radzi MA, Rezadad MI, Hajighorbani S. Power loss due to soiling on solar panel: A review. In: Renewable and sustainable energy reviews. 59. Elsevier Ltd; Jun-2016. p. 1307–16. https://doi.org/10.1016/j.rser.2016.01.044.
[47] Gilman P, Dobos A, Diorio N, Freeman J, Janzou S, Ryberg D. SAM photovoltaic model technical reference update. 2016.
[48] Perpiñán Ó. Energía solar fotovoltaica. 2018.

[49] Redweik P, Catita C, Brito M. Solar energy potential on roofs and facades in an urban landscape. Sol Energy Nov. 2013;97:332–41. https://doi.org/10.1016/j.solener.2013.08.036.
[50] van Sark WGJHM, Reich NH, Müller B, Armbruster A, Kiefer K, Reise C. Review of PV performance ratio development. World Renewable Energy Congress; 2012. p. 4795–800.
[51] Grupotech. Posibilidades de implantacion de instalaciones fotovoltaicas en la industria valenciana. 2011.
[52] Jordan DC, Kurtz SR. Photovoltaic degradation rates – an analytical review. Preprint; 2012.
[53] IDAE. Proyecto SECH-SPAHOUSEC. 2011.
[54] ANPIER. Anuario fotovoltaico. Asociación Nacional de Productores de Energía Fotovoltaica; 2019.
[55] de Madrid Cámara. Guía sobre empresas de servicios energéticos (ESE). Fundación de la Energía de la Comunidad de Madrid; 2010.
[56] Eléctrica de España Red. PVPC | ESIOS electricidad · datos · transparencia. 2018.
[57] Eléctrica de España Red. Análisis | ESIOS electricidad · datos · transparencia. 2019.
[58] Chase J. Trends in PV O&M pricing. 2018.
[59] inflation.eu, "Inflación histórica España – inflación histórica España IPC.".
[60] CNMC. Documento de consulta pública sobre la propuesta de metodología de cálculo de la tasa de retribución financiera de la actividad de producción de energía eléctrica a partir de fuentes de energía renovables, cogeneración y residuos para el siguiente periodo. 2018.
[61] Red eléctrica de España, "REData | red eléctrica de España." .
[62] PVSyst, "project design - carbon balance tool - detailed System LCE." .
[63] Chowdhury MS, et al. An overview of solar photovoltaic panels' end-of-life material recycling. Energy Strategy Rev Jan-2020;27:100431. https://doi.org/10.1016/j.esr.2019.100431. Elsevier Ltd.
[64] Atersa, "línea ULTRA - módulos fotovoltaicos - productos y servicios - atersa." .
[65] "G * Power 3.1 manual. 2017.
[66] Gatsonis C, Sampson AR. Multiple Correlation: Exact Power and Sample Size Calculations. Psychol Bull 1989;106(3):516–24. https://doi.org/10.1037/0033-2909.106.3.516.
[67] Cohen J. Statistical power analysis for the behavioral sciences. second ed..". Lawrence Erlbaum Associates; 1988.
[68] Banerjee A, Chitnis U, Jadhav S, Bhawalkar J, Chaudhury S. Hypothesis testing, type I and type II errors. Ind Psychiatr J 2009;18(2):127. https://doi.org/10.4103/0972-6748.62274.
[69] Aydin G. Modeling of energy consumption based on economic and demographic factors: The case of Turkey with projections. Renew Sustain Energy Rev 2014;35:382–9. https://doi.org/10.1016/j.rser.2014.04.004. Elsevier Ltd.
[70] Tabachnick BG. Experimental designs using ANOVA epidemiology and neurobehaviour of FASD in South Africa view project CyGaMEs view project. 2007.